

Laser Metal Deposition for Cladding

Subjects: Engineering, Manufacturing

Contributor: Jian Cheng, Yunhao Xing, Enjie Dong, Linjie Zhao, Henan Liu, Tingyu Chang, Mingjun Chen, Jinghe Wang, Junwen Lu, Jun Wan

With the development of society and the economy, there is an increasing demand for surface treatment techniques that can efficiently utilize metal materials to obtain good performances in the fields of mechanical engineering and the aerospace industry. The laser metal deposition (LMD) technique for cladding has become a research focus because of its lower dilution rate, small heat-effect zone and good metallurgical bonding between the coating and substrate.

Keywords: laser metal deposition (LMD) ; grain growth mechanism ; stress evolution

1. Mechanisms of Grain Growth in the Melt Pool

1.1. Melt Force Status

During the LMD process, the melt force status affects the melt flow direction in the melt pool and then affects the microstructure of the cladded layer, which ultimately determines the quality and performance of the cladded layer. Therefore, it is important to analyze the melt force status in the melt pool.

Li ^[1] indicated that in the laser cladding process, there are a variety of complex physical phenomena that work together, such as shielding gas conveying cladding powder, laser and powder interaction, powder and substrate melting, melt flows in the melt pool, heat conduction and so on. Thus, the melt force status in the melt pool is extremely complicated. In addition to gravity, the forces acting on the melt materials in the melt pool include: capillary pressure, Marangoni force, buoyancy, liquid flow viscous force, internal pressure of the melt pool caused by volume expansion, shielding gas pressure, powder impact force, etc. In the process of laser cladding, all the above-mentioned forces act together on the melting materials in the melt pool, so that the melt materials are in a complex flowing state in the melt pool.

1.2. Melt Flow Conditions

The flow of the melt materials in the melt pool is the result of the combined action of various forces, and it is also an important factor influencing the growth and formation of grains in the melt pool. Thus, in order to obtain an idealized grain morphology in cladded layers, it is necessary to understand the melt flow trend in the melt pool and the related factors that affect the melt flow.

In 2009, a 3D heat transfer model was developed by Kumar to simulate the LMD process. This model fully considers the complex physical phenomena (such as heat transfer, phase change and the addition of powder particles and fluid flow due to Marangoni–Rayleigh–Benard convection) in the LMD process. It is shown that surface-tension-driven Marangoni–Benard convection is dominant, and buoyancy-driven Rayleigh–Benard convection is insignificant ^[2]. Heiple et al. ^[3] proposed a mechanism to reveal the relationship between the surface tension temperature coefficient and the direction of melt flows. They indicated that if the surface tension temperature coefficient is negative ($\partial\sigma/\partial T < 0$

), the surface tension at the edge of the melt pool would be greater than the center tension of the melt pool. The free surface fluid of the melt pool flows from the center of the upper surface of the melt pool to the edge of the melt pool, and then flows into the bottom of the melt pool along the boundary of the melt pool. Finally, it flows upward near the center of the melt pool to form a reflux, and drives the internal melt materials to flow. On the contrary, if the surface tension temperature coefficient is positive ($\partial\sigma/\partial T > 0$

), the melt pool would form a clockwise circulation on the left side of the center line of the melt pool, and a counterclockwise circulation on the right side ^[4]. At this time, the melt pool flows downward to melt the substrate, making the melt pool deeper ^[4]. Gan et al. ^[4] studied the impact of the sulfur mass transport and the sulfur mass effects on the Marangoni flow using an improved 3D transient heat transfer and fluid flow numerical model. The results showed that the redistribution of sulfur would affect the state of the Marangoni flow, as the surface tension temperature coefficient changes

from positive to negative as the sulfur mass decreases in the clad layers. On the left side of the center line of the melt pool, the melt pool changes from a clockwise cycle to a counterclockwise cycle, which eventually causes the depth of the melt pool to change from deep to shallow. The sulfur concentration at the top surface of the clad layers increased 7 times as the mass flow rate decreased from 6 g/min to 0.1 g/min. There are two main flow patterns in the molten pool, that is, an outward flow pattern when the mass flow rate is high and a predominantly inward pattern when the mass flow rate is low. This is because when the sulfur mass flow rate is high, less of the substrate had been melted, and the concentration of the sulfur at the top of the clad layers was lower. Negative temperature coefficients of surface tension drive outward flows of melt in the molten pool.

Hu et al. [5] indicated that the melt pool shows an obvious inward flow pattern under the influence of the high sulfur content of Ti-15. In 2018, a high-energy synchrotron micro-radiography technique was used to observe the formation and flow state of melt pools during the laser cladding process by Aucott et al. [6], finding that adjusting the surface-active elements can be used to control the flow state of the internal metal melt. It is worth mentioning that the rare earth elements such as La and Ce are also surface-active elements [7][8][9], which can reduce the surface tension of the molten metal and improve its fluidity, thereby reducing the porosity in the clad layer and improving the hardness and wear resistance.

Therefore, in the process of LMD for cladding, the Marangoni double-ring vortex, which is affected by the surface tension gradient, can influence the depth of the melt pool by dominating the flow trend of the melt materials. In addition, the surface-active elements such as S, La and Ce can affect the surface tension temperature coefficient, thereby affecting the flow direction of the melt materials, and ultimately affecting the depth and shape of the melt pool.

1.3. Grain Morphology

In the LMD technology, the microstructure formed by the solidification of the substrate material and the powder directly affects the mechanical properties of the clad layer. The clad layer containing a large number of small equiaxed grains has characteristics of isotropy, good fatigue resistance and good wear resistance. The clad layer containing thick columnar grains has anisotropy and good high-temperature performance, but is prone to microcracks. Studying the morphology and forming process of grains in the microstructure of the clad layer is the prerequisite for exploring the mechanisms of crack formation and suppression methods, and it is also the basis for seeking ways to improve the performance of the workpiece, which is of great significance.

The morphology of metal crystals in the clad layer is mainly equiaxed grain and columnar grain. Wang et al. [10] revealed the grain morphology evolution behaviors of laser-deposited titanium alloy components via studying the influence of the mass deposition rate on the structure of the clad layer during the LMD layer-by-layer cladding process. They pointed out that there are two main solidification mechanisms in the LMD process, i.e., the upper part of the clad layer is mainly composed of small-sized equiaxed crystals, and the lower part of the clad layer is mainly composed of coarse columnar crystals produced by grain epitaxy; these two growth mechanisms compete with each other, which together determine the grain morphology of the clad layer. In addition, increasing the mass deposition rate would cause the expansion of the equiaxed grain area in the clad layer.

For the growth of columnar grains at the bottom of the melt pool during LMD, Henry et al. [11] pointed out that dendrites usually grow along the direction perpendicular to the substrate and closest to the direction of the heat flow $\langle 001 \rangle$. In 2016, Zhang et al. [12] pointed out that in the process of melt materials' solidification, most of the grains tend to grow along the $\langle 001 \rangle$ direction and form a grain boundaries misorientation angle of about 2° . However, in the bottom area of the melt pool, since the solid-liquid interface is arc-shaped, the dendrite growth is not strictly perpendicular to the surface of the substrate. This would cause the bottom grain boundary to be more disordered, and some grain sizes are smaller than other parts of the deposited layer. The hardness of different areas of the clad layer is different due to the changes in eutectic morphology, grain morphology distribution, grain boundaries misorientation and the precipitation of a small amount of strengthening phase in different areas.

When performing multi-layer laser cladding, there is a remelting phenomenon between two adjacent clad layers, which affects the growth of grains. Thijs et al. [13] indicated that in the laser additive manufacturing technology, the laser scanning strategies, which include raster, bi-directional, offset-out and fractal [14], can affect the grain growth direction by affecting the local heat transfer conditions, and ultimately can affect the microstructure. In the case of layer-by-layer cladding, due to the partial remelting of the previous layer, the columnar grains can grow further.

Therefore, in the melt pool of LMD, the crystal grain morphology is dominated by equiaxed grains on the surface of the melt pool and columnar grains at the bottom. The columnar grains grow at the bottom of the melt pool along the direction perpendicular to the solid-liquid interface and closest to the heat flow. When the multi-layer laser cladding is processed,

the equiaxed grains on the upper part of the melt pool in the previous cladded layer may be remelted, so that the columnar grains at the bottom of the melt pool can grow. It is worth noting that during the LMD process, the laser scanning strategy can affect the direction of grain growth by affecting the local heat transfer conditions, and ultimately affect the structure of the cladded layer.

1.4. Influence of Melt Flow on Grain Morphology

Since the melt materials are in a flowing state and the columnar grains at the bottom of the melt pool grow along the direction closest to the heat flow, the melt flow is directly related to the morphology of the crystal grains. Studying the influence of the melt flow on grain formation and growth is a prerequisite for regulating the formation of the microstructure of the cladded layer, and it is of great significance to improving the performance of the cladded layer.

In 2001, Canalis et al. ^[15] found that the flow of the melt pool contributes to dendrite fragmentation and the transport of dendrite arms; these dendrite arms and unmelted powder particles create a large number of nucleation sites for the solidification of the melt in the melt pool. Wang et al. ^[16] prepared Ni-based alloys on a single crystal substrate by LMD. They found that the flow field in the melt pool is an important factor that causes the deflection of dendrite growth during the layer-by-layer deposition process. Dendrites grow along the direction of the melt flow. In 2016, Chen et al. ^[17] studied the influence of the laser input angle on the dendritic microstructure, crystal orientation and the heat-affected zone (HAZ) liquation cracking tendency of Inconel 718 deposited on a polycrystalline substrate. They found that laser input angle can affect the growth of second dendrite arms, because adjusting the laser input angle can change the lateral temperature gradient, while at the same time, also making dendrites grow from [001] to [100] and can inhibit the formation of cracks in the heat-affected zone.

Similar grain morphologies were also found in LMD-fabricated Ti-based alloys ^{[10][18][19]}. There are few reports on the fabrication of Cu-based alloys by LMD technology. This is because the Cu element is usually present as a non-major element in the alloys (such as Al–Cu alloy, Al–Zn–Mg–Cu alloy) commonly used in LMD technology, so Cu-based alloys are not discussed here. Therefore, the melt flow in the melt pool has two main effects on the formation and growth of grains. On the one hand, the melt flow can promote the formation of equiaxed grains by breaking dendrites. On the other hand, the melt flow can affect the growth of columnar grains at the bottom of the melt pool by changing the direction of the heat flow. It should be noted that the grain morphologies in the LMD process are the result of a combination of factors such as the temperature conditions and melt flow in the molten pool.

1.5. Control the Cladding Microstructure by Coupling Physical Fields

In view of the fact that the melt flow in the melt pool has a direct impact on the formation and growth of crystal grains, the LMD process can be coupled with different physical fields such as high-frequency micro-vibration, ultrasonic vibration. So, the formation and growth of crystal grains would be affected to achieve the purpose of regulating the microstructure of the cladded layer.

In 2019, TiC/AlSi10Mg composite cladded layers were successfully fabricated on high-frequency microvibration platforms using the LMD process. During the solidification process, the long eutectic Si particles were broken by high-frequency vibrations and distributed uniformly with the flow of the melt. These broken eutectic Si particles serve as nucleation sites to form a fine net structure. The net structure and the α -Al phase are closely combined to form a dense microstructure ^[20].

In 2017, Cong et al. ^[21] combined ultrasonic vibrations with the laser-engineered net shape (LENS) process, finding that ultrasonic vibrations will generate periodic positive and negative pressure changes in the molten pool, thereby promoting the flow of the melt. This is due to the acoustic streaming and cavitation effects brought by ultrasonic vibrations, which generate instantaneous impact stress and temperature fluctuations in the melt pool, making the solidification front unstable. The broken grains flow back into the molten pool through the melt flow and become new nucleation sites, so the microstructure of the cladded layer changes from columnar grains to equiaxed grains ^[22].

Xie ^[23] introduced a pulse current into the laser cladding process and indicated that when the current passes through the melt, there would be an electromigration effect, Joule heating effect, Peltier effect, skin effect and hysteresis constriction effect. The introduction of a pulsed current can increase the degree of supercooling during metal solidification, thereby increase the nucleation rate and promote grain refinement ^[24]. In addition, different current densities in different regions of the metal melt would cause different shrinkage forces, resulting in a difference in the internal flow rate of the melt and shearing stress. If the shearing stress is large enough, the dendrites will be broken into nucleation sites for equiaxed grains, thereby promoting grain refinement ^[25].

In the research on the influence of magnetic fields on the solidification process of LMD, Li et al. [26] studied the effects of strong magnetic fields on the columnar-to-equiaxed transition (CET) during alloy solidification. They indicated that in the melt pool, the magnetic field interacts with the current generated by the flow of particles and the thermoelectric current generated by the thermoelectric effect to produce the Lorentz force and the thermoelectric magnetic force, respectively. The Lorentz force, thermoelectric magnetic force and magnetization force owing to the magnetic anisotropy of the dendrite work together on cells/dendrites and equiaxed grains, causing the cells/dendrites to break and driving the equiaxed grains to rotate to further destroy the cells/dendrites. Thus, applying a strong magnetic field during the solidification of the alloy would cause the fragmentation of cells/dendrites and the columnar-to-equiaxed transition. Zhao [27] applied the alternating magnetic field which is generated by a self-designed magnetic field device in the laser cladding process of Fe-based alloys. It was indicated that the electromagnetic stirring technology is based on two basic principles: first, Faraday's law of electromagnetic induction, that is, the conductive liquid generates an induced current when cutting the magnetic line of induction in a magnetic field; second, the charged body is subjected to an electromagnetic force in the magnetic field.

Coupling LMD technology with high-frequency micro-vibrations, ultrasonic vibrations, electric fields, magnetic fields and other physical fields is a feasible method to control the microstructure of the cladded layer. High-frequency micro-vibrations can increase the strength of the melt flow and break long strip dendrites. The ultrasonic vibrations promote the formation of a large number of equiaxed grains by acoustic streaming, cavitation and increasing the energy in the melt pool to increase the thermal gradient. The introduction of a current during the LMD process would cause a series of positive effects such as the electromigration effect, Joule heating effect, Peltier effect and so on, which will lead to grain refinement. The application of a strong magnetic field in the molten zone would generate a Lorentz force, thermoelectric magnetic force and magnetization force, which cause cells/dendrites to break and then the grains of the cladded layer to be refined.

In addition to the physical field-coupling technology, in recent years, cryogenic quenching to improve the performance of the cladding layer has begun to attract researchers' attention. Zhang et al. [28] quenched the deposited IN718-cladded layer in liquid nitrogen: the increased cooling rate reduced the segregation of niobium, and the aged hardness increased by 4%. In the research on the cryogenic quenching of Co-based [29] and Fe-based [30] alloys, the cryogenic initial temperature of the substrate dramatically reduced the clad dilution compared to a room temperature substrate. The hardness increased because of the reduction in the secondary dendrite arm's spacing.

In summary, in the LMD process for cladding, on the one hand, the melt materials in the melt pool are in a flowing state under the action of many forces, and the surface-active elements such as S, La and Ce can affect the surface tension temperature coefficient of the melt materials in the melt pool, thereby affecting the flow direction of the melt driven by the Marangoni double-ring vortex, and ultimately affecting the depth and shape of the melt pool. On the other hand, the grain morphology in the melt pool is dominated by equiaxed grains on the surface of the melt pool and columnar grains at the bottom. The number of equiaxed grains formed at the top of the melt pool is proportional to the nuclei density, and columnar grains grow at the bottom of the melt pool perpendicular to the solid-liquid interface and along the direction closest to the heat flow. The nuclei density affecting the distribution of equiaxed grains is related to two phenomena: part of the cladding powder is unmelted, and the melt flow breaks dendrites in the melt pool. The laser scanning strategy, the laser input angle and other factors can affect the direction of the heat flow in the melt pool to affect the direction of grain growth, and ultimately can affect the microstructure of the cladded layer. In addition, when the solid-liquid interface at the bottom of the melt pool is irregular, the dendrite growth direction at the bottom of the melt pool would not be perpendicular to the substrate, resulting in smaller grain sizes at the bottom of the melt pool and more disordered grain boundaries. When performing multi-layer laser cladding processing, the equiaxed grains on the upper part of the melt pool in the previous cladded layer can be remelted by changing the process parameters, so that the columnar grains at the bottom of the melt pool can grow further. Thus, the melt flow in the melt pool has two main effects on the formation and growth of grains. On the one hand, the melt flow can promote the formation of equiaxed grains by breaking dendrites. On the other hand, the melt flow can affect the growth of columnar grains at the bottom of the melt pool by changing the direction of the heat flow. When the LMD technology is coupled with high-frequency micro-vibrations, ultrasonic vibrations, electric fields, magnetic fields and other physical fields, different physical fields directly or indirectly affect the melt flow and break the crystal grains in the melt pool to cause the expansion of the equiaxed grain area in the cladded layer, thereby realizing the control of the microstructure of the cladded layer. The study of the influence of the melt flow on grain morphology is the basis for studying the control of the microstructure of the cladded layer by coupling different physical fields. Only by understanding the grain growth mechanism in the melt pool can researchers further explore the direct causes of defects and formulate methods to suppress cladding defects from the perspective of the microstructure, so as to obtain a cladded layer with excellent performance.

2. Distribution and Evolution of Temperature and Stress

2.1. Distribution and Evolution of Temperature

In the LMD process, the high-temperature area near the heat source has a very obvious temperature gradient, and the cladded layer being processed by the laser would affect the thermal history of the nearby cladded layer and then affect the formation of the cladded layer microstructure in the nearby area.

In terms of heat transfer, during the laser cladding process, the substrate near the cladding area is preheated by heat conduction. When the laser scans to this point, the temperature reaches the maximum value. After the laser leaves this point, the workpiece dissipates heat through the substrate heat conduction, cladded layer surface and air convection and heat radiation, so the temperature drops sharply [31][32]. The temperature of this point would rise and fall again when performing the next cladding tracks.

The simulation analysis of the LMD process shows that the temperature gradient near the laser heat source is large. The previous cladding track not only preheats the latter cladding track, but also cyclically heats the adjacent cladding tracks of the previous layer. Therefore, the temperature evolution process of the overlap area and the adjacent area of the LMD-cladded layer would lead to heat treatment or solid-state phase transitions, which causes microstructure evolution and thermal–mechanical interactions, such as thermal warpage and residual stress formation. In addition, in the process of multi-layer (long-time heating) or large-area laser cladding, the warpage or deformation of the substrate due to thermal stress on the substrate cannot be ignored. Usually, this adverse effect can be improved by adding water cooling channels under the substrate or adopting intermittent cladding.

2.2. Distribution and Evolution of Stress

The analysis of the stress composition, distribution and evolution of the cladded layer prepared by LMD technology is the basis for further exploring the causes of cracks perpendicular to the scanning direction in the cladded layer.

In the LMD process, on the one hand, due to the difference between the thermal and physical properties of the cladding material and the substrate, such as the thermal expansion coefficient, thermal conductivity, etc., the temperature distribution in the cladding area would be uneven, which will affect the generation and distribution of thermal stress. At the same time, due to the large temperature gradient, there will be some phase changes in the overlap zone and the heat-affected zone, resulting in compressive or tensile stress. On the other hand, plastic strain, elastic strain and thermal strain mainly occur in the cladding area. Among them, the change in plastic strain is not significant. The elastic strain firstly drops to a negative value, and then increases to a positive value during the cooling process and remains unchanged. The thermal strain has a peak when the laser beam passes, and then gradually decreases as the melt materials cool down [33]. The residual stress refers to the stress that an object has in a state of mechanical and thermal equilibrium in the absence of an external force. Therefore, the residual stress produced by the cladding process is mainly composed of compression or tensile stress and thermal stress. The residual strain is composed of elastic strain and thermal strain.

For the relationship between stress and strain, Zhang et al. [34] used the finite element method to simulate the distributions of the temperature field and stress field in the LMD process. It was indicated that because the length of the substrate along the laser scanning direction is greater than the width along the direction perpendicular to the laser scanning direction and the thickness of the substrate, the workpiece undergoes the greatest deformation resistance along the laser scanning direction after cladding. The strain distribution in the three directions near the junction of the cladded layer and the substrate is as follows: the strain along the thickness of the substrate is greater than the strain in the transverse direction (perpendicular to the scanning direction) and greater than the strain in the longitudinal direction (scanning direction). Correspondingly, the residual stress distribution in these three directions is as follows: the residual stress in the thickness direction of the substrate is smaller than the transverse residual stress and smaller than the longitudinal residual stress [29]. Thus, the maximum residual tensile stress along the scanning direction is the main cause of cracks in the cladded layer perpendicular to the scanning direction.

When performing single-track or multi-track laser cladding, the stress evolution process of the cladded layer is slightly different, but the stress distribution is roughly the same. For single-track laser cladding, Farahmand et al. [33] pointed out that according to the Von Mises stress distribution, the high stress concentration of laser cladding mainly exists in the cladding zone (CZ) and the heat-affected zone (HAZ). The cladding zone (CZ) and the interfacial zone (IZ) are high tensile stress zones, and the heat-affected zone (HAZ) is a compressive stress zone [35]. The generation of the residual compressive stress of the substrate is caused by the substrate material undergoing a phase change (such as martensite,

etc.) when the laser heat source acts, thereby generating additional compressive stress. At the same time, due to the mechanical balance, the compressive stress of the substrate also increases the tensile stress in the clad layer.

As the melt materials in the melt pool melt and solidify, the stress in the cladding zone (CZ) is constantly changing. In 2015, Dai et al. [36] used the finite element method to simulate the temperature field and stress field of the ring laser cladding process on Inconel 718 Ni-based alloys. They found that during the heating process, the cladding metal is subjected to certain circumferential (scanning direction) and radial (perpendicular to the scanning direction) compressive stress within a certain temperature range due to heating. When the temperature reaches a certain value, the stress on the cladding metal almost becomes zero. When the cladding metal is cooled and solidified, the stress on it at the beginning is very small. When the temperature reaches a certain value, the stress in the circumferential and radial directions begins to appear as tensile stress. If the tensile stress of the cladding metal is greater than its plasticity, the cracks may occur.

It is worth mentioning that in addition to the thermal history and phase transition of the clad layer, the cause of residual stress is also related to the thermal conductivity, thermal expansion coefficient, Young's modulus and yield stress of the substrate material and alloy powder, as well as the geometric shape of the workpiece, the processing parameters, the scanning strategy and other factors. Thus, selecting a powder material with a thermal expansion coefficient similar to that of the substrate, selecting a suitable LMD scanning strategy, preheating the substrate, reducing the laser power and increasing the laser scanning speed can reduce the residual stress of the clad layer [33][35][37]. One of the important reasons for the stress in the laser-clad layer is the large difference between the thermal expansion coefficient of the cladding alloy and the substrate. So, a reasonable choice of alloy powder with a thermal expansion coefficient similar to the substrate is a way to reduce the residual stress of the clad layer and reduce its crack sensitivity. Dai et al. [38] used finite element analysis to study the effect of the laser scanning strategy on the residual stress and deformation of the clad layer. They found that by using the offset-out scanning strategy, the residual stress can be reduced to one third of the residual stress produced by the bi-directional scanning strategy. In 2017, Yang et al. [39] indicated that laser cladding can reduce the residual stress between the clad layer and the copper substrate by preheating, which can also suppress the occurrence of cracks.

Therefore, in the LMD process, the residual stress is mainly composed of compressive or tensile stress and thermal stress, while the residual strain is composed of elastic strain and thermal strain. The relationship between stress and strain is affected by the structure of the substrate. Along the direction where the deformation resistance of the substrate is greatest, the strain is the smallest, the residual stress is the largest and the cracks are most likely to occur. The cladding zone (CZ) and the interfacial zone (IZ) are tensile stress zones, and the heat-affected zone (HAZ) is a compressive stress zone. The interfacial zone (IZ) stress concentration is higher, and it is more sensitive to crack formation. In multi-track laser cladding, the previous cladding track has relatively low residual stress due to the cyclic heating and cooling effects of the subsequent cladding track. During laser processing, the cladding metal is firstly subjected to compressive stress. Then, the stress becomes zero as the temperature rises. Finally, as the molten metal cools and solidifies, tensile stress appears in the scanning direction and the direction perpendicular to the scanning direction. If the tensile stress is greater than the plasticity of the cladding metal, cracks will occur. In addition, the generation of residual stress is also related to the thermal conductivity, thermal expansion coefficient, Young's modulus, and yield stress of the substrate material and alloy powder, as well as the part's geometry, processing parameters, scanning strategy and other factors. Selecting powder materials with a thermal expansion coefficient similar to the substrate, selecting a suitable LMD scanning strategy, preheating the substrate, reducing the laser power and increasing the laser scanning speed can reduce the residual stress of the clad layer, thereby reducing the crack sensitivity of the clad layer.

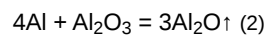
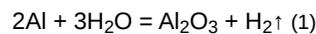
In summary, in addition to the obvious temperature gradient near the heat source, the difference between the thermal and physical properties of the cladding material and the substrate, such as the thermal expansion coefficient, thermal conductivity, etc., as well as the processing parameters and scanning strategy can cause an uneven temperature distribution in the laser cladding area, thereby affecting the generation and distribution of thermal stress. Moreover, different areas of the clad layer have different thermal histories directly related to the temperature field, so there will be different phase transitions in the cladding zone (CZ), the interfacial zone (IZ), HAZ and overlap areas, resulting in tensile or compressive stress. The thermal stress and tensile or compressive stress together constitute residual stress. The relationship between stress and strain is affected by the structure of the substrate. Along the direction where the deformation resistance of the substrate is greatest, the strain is the smallest, the residual stress is the largest and the cracks are most likely to occur. There are several potential ways to reduce the residual stress of the clad layer: selecting powder materials with a thermal expansion coefficient similar to the substrate, selecting a suitable LMD scanning strategy, preheating the substrate and adjusting the process parameters to reduce the laser energy density. Therefore, studying the distribution and evolution of temperature and stress can further reveal the formation mechanism and hence facilitate the development of defect suppression methods for obtaining well-performing clad layers.

3. Defect Formation and Suppression

3.1. Causes of Pore Formation

Porosity is a key factor for some problems such as stress concentration, performance degradation and so on [40]. Thus, in order to prepare cladded layers with good performances, it is necessary to explore the direct causes of pore formation. Only by understanding the reasons for pore formation can researchers further develop methods to suppress pores.

In 2019, Zhang et al. [41] pointed out in comparative experiments of laser welding and tungsten inert gas welding (TIG) between laser selective cladding and cast AISi10Mg that the oxygen content in the laser selective cladding AISi10Mg plate is much higher than that in the as-cast AISi10Mg plate. Oxides easily absorb water and protective gas in the air and induce reaction (1) under the laser action. The solubility of hydrogen in liquid aluminum can reach 0.7 mL/(100 mg), while that in solid aluminum is only 0.036 mL/(100 mg). So, the hydrogen generated by aluminum and water under the laser action is precipitated during the process of aluminum alloy changing from liquid to solid, resulting in the generation of pores. As for the oxide Al_2O_3 , it can be seen as an oxide film on the powder or substrate. The oxide film usually causes irregular pores of about tens of microns in the cladded layer [42]. However, when Liao et al. [43] studied the mechanism of alumina loss in laser selective cladding of Al_2O_3 -AISi10Mg composites, it was found that excessively high temperatures in the melt pool during cladding will cause the reduction reaction of aluminum to alumina in the melt pool (2), resulting in pores in the cladded layer.



The LMD processing parameters can directly or indirectly affect the melt flow in the melt pool so as to affect pore formation. Ng et al. [44] discussed the relationship between LMD process parameters and porosity in studying the formation of pores and bubble retention during the LMD process. As the laser power increases, the porosity first decreases and then increases. It was found that an increase in laser power will increase the input heat and reduce the solidification rate, allowing bubbles to escape before the melt materials in the melt pool solidify, and it will also reduce the pores caused by insufficient melted powder [45]. However, if the laser power is too high, the melt flow in the melt pool will be more violent and will aggravate the powder, trapping the shielding gas and bringing it into the melt pool to form pores, which is also the reason for the increase in the porosity caused by the increase in the powder feeding rate. It is worth mentioning that the effect of the Marangoni flow on driving the flow of bubbles is 5 times the effect of the floating bubbles themselves, so the Marangoni flow will cause bubbles to deposit at the bottom of the melt pool or promote bubbles to coalesce when the melt flows, causing bubbles to aggregate and produce large pores. Kumar et al. [46] pointed out that in the laser additive manufacturing of Inconel 718, choosing the right hatch distance can help reduce the porosity between two adjacent cladded layers through remelting. However, in 2019, Langebeck et al. [47] found that the oxide layer on the surface of the aluminum alloy will produce a chemical reaction during the LMD process, and the gas produced in this chemical reaction causes the pore volume to increase as the hatch distance increases.

3.2. Methods of Pore Suppression

Understanding the direct causes of pore formation, it has become a current research hotspot to develop corresponding pore suppression methods. In LMD for cladding, the use of effective methods to suppress pores can greatly reduce the stress concentration and improve the performance of the workpiece, which is of great significance for further research on the performance of cladded layers prepared by various powders.

Firstly, the low-porosity powder can be used to obtain a low-porosity cladded layer. Zhao et al. [48] used LRF technology to deposit Inconel 718 powders. They found that the powder material produced by plasma rotating electrode preparation (PREP) has a lower porosity compared with the gas atomized powder.

Secondly, the porosity of the cladded layer can also be reduced by changing the chemical reaction in the melt pool to inhibit the generation of reaction gas. In 2019, Kang et al. [49] promoted the reaction of oxygen and Cr by adding an appropriate amount of Cr particles to the alloy steel powder, thereby inhibiting the carbon-oxygen reaction which could generate gas in the molten pool, thus reducing the porosity of the cladded layer. Li [50] indicated that by baking the powder before LMD, the moisture on the powder's surface can be dried. This method can not only reduce the porosity caused by the evaporation of water during processing, but also reduce the porosity by inhibiting the chemical reaction of the aluminum alloy powder with water under the laser action. In 2014, Alshaer et al. [51] found that short pulse laser surface cleaning can be used to reduce the porosities of the AC170 PX aluminum-welded coating layers.

Finally, selecting appropriate LMD process parameters, such as laser power, powder feeding rate, scanning speed, etc. [44][46], and remelting processes can also reduce the porosity of the clad layer. Gao et al. [52] indicated that the remelting process can not only remove pores, but also improve the surface finish of the clad layer. It is interesting to note that the heat-treatment-related process does not have a large effect on the porosity.

In addition, coupling some physical fields with LMD technology can also reduce the generation of pores. Zhou et al. [53] found that in the LMD process, the application of an electromagnetic force can effectively prevent the appearance of welding pores. In 2018, Zhang et al. [54] combined electric-magnetic compound fields and laser cladding technology, and the results showed that a downward Ampere force can reduce the porosity and the size of the pore. Li et al. [20] indicated that the application of appropriate high-frequency micro-vibrations in laser processing can intensify the flow of the melt materials, thereby promoting the floating of gas and slag in the melt pool, and ultimately achieving the effect of reducing the porosity.

Therefore, corresponding to the reasons for the formation of pores in the LMD process, the methods to reduce the porosity of the processed workpiece mainly include using low porosity powder, inhibiting the chemical reaction of gas generated in the LMD process, choosing the appropriate LMD process parameters or adopting the remelting process method. In addition, coupling some physical fields with LMD can also reduce the generation of pores by affecting the melt flow.

3.3. Causes of Crack Formation

In the clad layer prepared by LMD, the cracks are considered to be the worst defects because they directly cause the workpiece to fail. Crack sensitivity can be described as the crack initiation probability of the clad layer. For a laser-clad layer, the cracks are usually perpendicular to the scanning direction [55]. In order to develop methods to suppress the formation of cracks to improve the quality of the clad layer, it is necessary to explore the crack formation mechanisms.

The cracks in the LMD-clad layer can be divided into hot cracks and cold cracks. The initiation of hot cracks is caused by hot tearing and is affected by the microstructure [55][56]. The cold cracks refer to the cracks caused by the phase transition when the material is heated and cooled to a lower temperature, and also refer to the cracks caused by the excessive thermal strain during melting and solidification due to the different thermal characteristics of the cladding material and the substrate. The cold cracks mainly occur in the heat-affected zone (HAZ) of the clad layer [57].

The segregation phenomenon and the uneven distribution of compounds, coarse brittle phases and impurities in the clad layer are important factors for the formation of hot cracks [55][56][58][59]. In 2018, Wang et al. [55] found that V_2O_5 can be used as a grain refiner of NiCrBSiC laser-clad layers. The addition of V_2O_5 inhibits the formation of brittle phases and promotes the uniform distribution of most elements and compounds to reduce crack sensitivity. Moreover, the segregation phenomenon in the alloy liquid film between dendrites in the clad layer is also an important factor leading to cracks. In 2016, Cloots et al. [56] indicated that there is a low-melting, high-concentration Zr liquid film near the crystal grains formed in the cladding zone (CZ), which leads to brittle grain boundaries, and these brittle grain boundaries cannot transmit residual stress and cause cracks. In 2020, Alizadeh-Sh et al. [58] fabricated Inconel 718 laser cladding coating on an A-286 Fe-based superalloy substrate. They found that the dilution rate and impurity elements such as S and P can affect the segregation of dendrites so as to cause cracks. The higher the segregation potential of the alloying elements, the more prone is the substrate to solidification cracks. Nakki et al. [60] found that Inconel 625 with a lower impurity content (such as S, P, B) was the least prone to hot cracking. In addition, the thicker the dendrites are, the more likely the alloy liquid will penetrate between the dendrites, which would lead to an increase in the thickness of the intergranular liquid film, and hence a decrease in the critical thermal stresses [61].

Therefore, the cracks in the LMD-clad layer can be divided into hot cracks and cold cracks. The initiation of hot cracks is generally caused by hot tearing, which is directly related to the segregation phenomenon and the uneven distribution of compounds, coarse brittle phases and impurities in the clad layer. However, for the initiation of cold cracks, they are generally caused by the phase transition in the heat-affected zone (HAZ) of the clad layer.

3.4. Methods of Crack Suppression

In order to prepare laser-clad workpieces with good quality and high reliability, suppressing the formation of cracks in the clad layer has become the current research frontier of LMD technology. Due to the different causes of cold cracks and hot cracks, the methods for reducing crack sensitivity are also different.

For cold cracks, the method of preheating the substrate can be used to reduce the crack sensitivity of the heat-affected zone (HAZ) in the substrate. In 2020, Bidron et al. [57] proposed that, compared to the substrate without induction preheating, the induction preheating of the substrate can change the precipitated phases in the substrate, thereby reducing the crack sensitivity of the HAZ. It is worth noting that appropriately reducing the power input or increasing the laser scanning speed can also reduce the crack sensitivity of the heat-affected zone (HAZ) [62].

For hot cracks, the crack sensitivity of the cladded layer can be reduced by refining the grains of the cladded layer. There are three main methods for refining the grains of the cladded layer: controlling the process parameters, coupling the physical fields, and adding rare earth powders.

Different alloy powders have different microstructures under the same process parameters. In general, however, when the lower laser power and higher scanning speed are combined, a finer microstructure in the cladded layer is usually formed due to the low input energy and high cooling rate, while a higher laser power and lower scanning speed will increase the incident energy and reduce the cooling rate, resulting in a coarser microstructure in the cladded layer [13][44][46][62]. Furthermore, increasing the powder feeding rate will cause the unmelted powder to become nucleation sites for equiaxed grains and hence refine the microstructure of the cladded layer [10]. Coupling the LMD process with different physical fields, such as high-frequency vibrations [20], ultrasonic vibrations [21][22], electric fields [23], magnetic fields [26][27], etc., can promote the refinement of the crystal grains in the melt pool by breaking dendrites, thereby reducing the crack sensitivity of the cladded layer. Another method for refining the grains of the cladded layer is to add rare earth powder to the processed alloy powder. In 2020, Opprecht et al. [63] added various quantities of Yttrium Stabilized Zirconia (YSZ) to an Al6061 powder to form Al_3Zr as the nucleation sites for equiaxed grain in a molten state to induce grain refinement and suppress the formation of columnar grains and hence eliminate the hot cracks of the 6061 alloy in laser cladding. The experimental results showed that as the amount of YSZ increases, the equiaxed grain zone extends to the center of the melt pool. Meanwhile, the length and number of cracks in the cladding zone are significantly reduced or even eliminated. Wang et al. [5] indicated that La, as a surface-active element, is mainly distributed on the grain boundaries, and that the use of La_2O_3 is beneficial to refine the grains and microstructure of the Fe-based cladded layer under oil lubrication condition.

In the LMD process, in order to suppress the formation of cold cracks, a method of preheating the substrate can be used, while in order to suppress the formation of hot cracks, the goal is mainly achieved by refining the grains of the cladded layer. The methods of refining the grains of the cladded layer mainly include three methods: changing the process parameters, adding physical fields to the LMD technology and adding rare earth materials in the powder.

It should be noted that the roughness has an important influence on the wear resistance and corrosion resistance of the cladded layer. Chen et al. [64] showed that the cladding speed has a significant effect on the surface quality. Generally, the roughness decreased with the increase in the scanning speed. In addition, a high overlap rate reduced the surface fluctuation of the coating and improved the surface quality of the cladded layer. Therefore, the roughness of the cladded layer can be improved by optimizing the process parameters. In occasions with high requirements or roughness, high-quality cladded surfaces can be obtained by post-machining methods.

To sum up, the most important defects in the cladded layer of LMD technology are pores and cracks. The formation of pores is related to the hollow powder, physical and chemical reactions in the laser cladding process, and cladding process parameters. Improving powder quality and optimizing process parameters can suppress the formation of pore defects. At the same time, external field aids such as electromagnetic fields and ultrasonic vibrations have shown good effects in suppressing pore defects, and will be a hot research direction in the future. The formation of crack defects is closely related to the difference in the thermal expansion characteristics of powder materials and substrate materials, phase distribution and element segregation. Preheating the substrate can reduce the generation of cold cracks, and the use of inoculants such as rare earth powders can refine the grains and significantly reduce the formation of hot cracks; it is considered to be one of the most effective methods to suppress hot crack defects, and has begun to attract more and more researchers' attention.

References

1. Li, J. Research on the geometrical feature and the molten pool's surface tension of laser cladding layer. Master's Thesis, Yanshan University, Qinhuangdao, China, 2014.
2. Kumar, A.; Roy, S. Effect of Three-Dimensional Melt Pool Convection on Process Characteristics During Laser Cladding. *Comput. Mater. Sci.* 2009, 46, 495–506.

3. Heiple, C.R.; Roper, J.R. Mechanism for Minor Element Effect on GTA Fusion Zone Geometry. *Weld. J.* 1982, 61, 97–102.
4. Gan, Z.; Yu, G.; He, X.; Li, S. Surface-Active Element Transport and its Effect on Liquid Metal Flow in Laser-Assisted Additive Manufacturing. *Int. Commun. Heat Mass Transf.* 2017, 86, 206–214.
5. Hu, Y.; Wang, G.; Ye, M.; Wang, S.; Wang, L.; Rong, Y. A precipitation hardening model for Al-Cu-Cd alloys. *Mater. Des.* 2018, 151, 123–132.
6. Aucott, L.; Dong, H.; Mirihanage, W.; Atwood, R.; Kidess, A.; Gao, S.; Wen, S.; Marsden, J.; Feng, S.; Tong, M.; et al. Revealing Internal Flow Behaviour in Arc Welding and Additive Manufacturing of Metals. *Nat. Commun.* 2018, 9, 5414.
7. Sun, S.; Fu, H.; Ping, X.; Guo, X.; Lin, J.; Lei, Y.; Wu, W.; Zhou, J. Effect of CeO₂ Addition On Microstructure and Mechanical Properties of In-Situ (Ti, Nb)C/Ni Coating. *Surf. Coat. Technol.* 2019, 359, 300–313.
8. Wang, W.J.; Fu, Z.K.; Cao, X.; Guo, J.; Liu, Q.Y.; Zhu, M.H. The Role of Lanthanum Oxide on Wear and Contact Fatigue Damage Resistance of Laser Cladding Fe-based Alloy Coating Under Oil Lubrication Condition. *Tribol. Int.* 2016, 94, 470–478.
9. Zhang, X.; Liu, H.; Jiang, Y.; Wang, C. Research Progress of Functional Composite Coatings on Ti6Al4V Alloy Surface Prepared by Laser Cladding Technique. *Rare Met. Mater. Eng.* 2012, 41, 178–183.
10. Wang, T.; Zhu, Y.Y.; Zhang, S.Q.; Tang, H.B.; Wang, H.M. Grain Morphology Evolution Behavior of Titanium Alloy Components During Laser Melting Deposition Additive Manufacturing. *J. Alloys Compd.* 2015, 632, 505–513.
11. Gäumann, M.; Henry, S.; Cléton, F.; Wagnière, J.-D.; Kurz, W. Epitaxial Laser Metal Forming: Analysis of Microstructure Formation. *Mater. Sci. Eng. A* 1999, 271, 232–241.
12. Zhang, Y.; Yang, L.; Dai, J.; Huang, Z.; Meng, T. Grain Growth of Ni-based Superalloy IN718 Coating Fabricated by Pulsed Laser Deposition. *Opt. Laser Technol.* 2016, 80, 220–226.
13. Thijs, L.; Verhaeghe, F.; Craeghs, T.; Van Humbeeck, J.; Kruth, J.P. A Study of the Microstructural Evolution During Selective Laser Melting of Ti–6Al–4V. *Acta Mater.* 2010, 58, 3303–3312.
14. Yu, J.; Lin, X.; Ma, L.; Wang, J.; Fu, X.; Chen, J.; Huang, W. Influence of Laser Deposition Patterns on Part Distortion, Interior Quality and Mechanical Properties by Laser Solid Forming (LSF). *Mater. Sci. Eng. A* 2011, 528, 1094–1104.
15. Gäumann, M.; Bezencon, C.; Canalis, P.; Kurz, W. Single-Crystal Laser Deposition of Superalloys: Processing-Microstructure Maps. *Acta Materialia* 2001, 49, 1051–1062.
16. Wang, G.; Liang, J.; Zhou, Y.; Zhao, L.; Jin, T.; Sun, X. Variation of Crystal Orientation During Epitaxial Growth of Dendrites by Laser Deposition. *J. Mater. Sci. Technol.* 2018, 34, 732–735.
17. Chen, Y.; Lu, F.; Zhang, K.; Nie, P.; Hosseini, S.R.E.; Feng, K.; Li, Z.; Chu, P. Investigation of Dendritic Growth and Liquation Cracking in Laser Melting Deposited Inconel 718 at Different Laser Input Angles. *Mater. Des.* 2016, 105, 133–141.
18. Saboori, A.; Gallo, D.; Biamino, S.; Fino, P.; Lombardi, M. An Overview of Additive Manufacturing of Titanium Components by Directed Energy Deposition: Microstructure and Mechanical Properties. *Appl. Sci.* 2017, 7, 883.
19. Zhang, F.; Qiu, Y.; Hu, T.; Clare, A.T.; Li, Y.; Zhang, L.-C. Microstructures and Mechanical Behavior of Beta-Type Ti-25V-15Cr-0.2Si Titanium Alloy Coating by Laser Cladding. *Mater. Sci. Eng. A* 2020, 796, 140063.
20. Li, C.; Sun, S.; Liu, C.; Lu, Q.; Ma, P.; Wang, Y. Microstructure and Mechanical Properties of TiC/AlSi10Mg Alloy Fabricated by Laser Additive Manufacturing Under High-Frequency Micro-Vibration. *J. Alloys Compd.* 2019, 794, 236–246.
21. Cong, W.; Ning, F. A Fundamental Investigation on Ultrasonic Vibration-Assisted Laser Engineered Net Shaping of Stainless Steel. *Int. J. Mach. Tools Manuf.* 2017, 121, 61–69.
22. Zhang, S.; Zhao, Y.; Cheng, X.; Chen, G.; Dai, Q. High-Energy Ultrasonic Field Effects on the Microstructure and Mechanical Behaviors of A356 Alloy. *J. Alloys Compd.* 2009, 470, 168–172.
23. Xie, D.; Zhao, J.; Qi, Y.; Li, Y.; Shen, L.; Xiao, M. Decreasing pores in a laser clad layers with pulsed current. *Chin. Opt. Lett.* 2013, 11, 111401.
24. Barnak, J.P.; Sprecher, A.F.; Conrad, H. Colony (Grain) Size Reduction in Eutectic TiC Pb-Sn Castings by Electroplusing. *Scr. Metallurgica Mater.* 1995, 32, 879–884.
25. Nakada, M.; Shiohara, Y.; Flemings, M.C. Modification of Solidification Structures by Pulse Electric Discharging. *ISIJ Int.* 1990, 30, 27–33.
26. Li, X.; Gagnoud, A.; Fautrelle, Y.; Ren, Z.; Moreau, R.; Zhang, Y.; Esling, C. Dendrite Fragmentation and Columnar-To-Equiaxed Transition During Directional Solidification at Lower Growth Speed Under a Strong Magnetic Field. *Acta*

27. Zhao, D.; Xu, L.; Fu, Y. Effects of molecule force on free vibration for a micro electromagnetic harmonic drive system. *Mech. Ind.* 2021, 22, 12.
28. Zhang, Y.; Li, Z.; Nie, P.; Wu, Y. Effect of ultrarapid cooling on microstructure of laser cladding IN718 coating. *Surf. Eng.* 2013, 29, 414–418.
29. Lisiecki, A.; Slizak, D.; Kukofka, A. Laser cladding of co-based metallic powder at cryogenic conditions. *J. Achiev. Mater. Manuf. Eng.* 2019, 1, 20–31.
30. Lisiecki, A.; Slizak, D. Hybrid laser deposition of fe-based metallic powder under cryogenic conditions. *Metals* 2020, 10, 190.
31. Zhou, J.; Qiu, C.J.; Cheng, X.Y. Finite Finite Element Simulation of Temperature Field on Laser Cladded layers Regulated by Micro-forging. *Adv. Mater. Res.* 2011, 328, 1417–1420.
32. Anusha, E.; Kumar, A.; Shariff, S. A novel method of laser surface hardening treatment inducing different thermal processing condition for Thin-sectioned 100Cr6 steel. *Opt. Laser Technol.* 2020, 125, 106061.
33. Farahmand, P.; Kovacevic, R. An Experimental–Numerical Investigation of Heat Distribution and Stress Field in Single- and Multi-Track Laser Cladding by a High-Power Direct Diode Laser. *Opt. Laser Technol.* 2014, 63, 154–168.
34. Zhang, Q.; Xu, P.; Zha, G.; Ouyang, Z.; He, D. Numerical simulations of temperature and stress field of Fe-Mn-Si-Cr-Ni shape memory alloy coating synthesized by laser cladding. *Optik* 2021, 242, 167079.
35. Liu, H.; Qin, X.; Wu, M.; Ni, M.; Huang, S. Numerical Simulation of Thermal and Stress Field of Single-Track Cladding in Wide-Beam Laser Cladding. *Int. J. Adv. Manuf. Technol.* 2019, 104, 3959–3976.
36. Dai, D.P.; Jiang, X.H.; Cai, J.P.; Lu, F.; Chen, Y.; Li, Z.G.; Deng, D. Numerical Simulation of Temperature Field and Stress Distribution in Inconel718 Ni Base Alloy Induced by Laser Cladding. *Chin. J. Laser* 2015, 42, 121–128.
37. Kattire, P.; Paul, S.; Singh, R.; Yan, W. Experimental Characterization of Laser Cladding of CPM 9V On H13 Tool Steel for Die Repair Applications. *J. Manuf. Process.* 2015, 20, 492–499.
38. Dai, K.; Shaw, L. Distortion Minimization of Laser-Processed Components through Control of Laser Scanning Patterns. *Rapid Prototyp. J.* 2002, 8, 270–276.
39. Yang, X.; Zeng, R.; Fu, X.; Wang, X.; Zhou, J.; Yu, L. Influence of the Cu content on the electrochemical corrosion performances of Ni60 coating. *Corros. Sci.* 2022, 22, 110408.
40. Choo, H.; Sham, K.-L.; Bohling, J.; Ngo, A.; Xiao, X.; Ren, Y.; Depond, P.J.; Matthews, M.J.; Garlea, E. Effect of Laser Power on Defect, Texture, and Microstructure of a Laser Powder Bed Fusion Processed 316L Stainless Steel. *Mater. Des.* 2019, 164, 107534.
41. Zhang, C.; Bao, Y.; Zhu, H.; Nie, X.; Zhang, W.; Zhang, S.; Zeng, X. A Comparison Between Laser and TIG Welding of Selective Laser Melted AlSi10Mg. *Opt. Laser Technol.* 2019, 120, 105696.
42. Tang, M.; Chris Pistorius, P. Oxides, Porosity and Fatigue Performance of AlSi10Mg Parts Produced by Selective Laser Melting. *Int. J. Fatigue* 2017, 94, 192–201.
43. Liao, H.; Zhu, H.; Xue, G.; Zeng, X. Alumina Loss Mechanism of Al₂O₃-AlSi₁₀ Mg Composites During Selective Laser Melting. *J. Alloys Compd.* 2019, 785, 286–295.
44. Ng, G.K.L.; Jarfors, A.E.W.; Bi, G.; Zheng, H.Y. Porosity Formation and Gas Bubble Retention in Laser Metal Deposition. *Appl. Phys. A* 2009, 97, 641–649.
45. Fu, Y.; Lored, A.; Martin, B.; Vannes, A.B. A Theoretical Model for Laser and Powder Particles Interaction During Laser Cladding. *J. Mater. Processing Technol.* 2002, 128, 106–112.
46. Kumar, P.; Farah, J.; Akram, J.; Teng, C.; Ginn, J.; Misra, M. Influence of Laser Processing Parameters on Porosity in Inconel 718 During Additive Manufacturing. *Int. J. Adv. Manuf. Technol.* 2019, 103, 1497–1507.
47. Langebeck, A.; Bohlen, A.; Freisse, H.; Vollertsen, F. Additive Manufacturing with the Lightweight Material Aluminium Alloy EN AW-7075. *Weld. World* 2020, 64, 429–436.
48. Zhao, X.; Chen, J.; Lin, X.; Huang, W. Study on Microstructure and Mechanical Properties of Laser Rapid Forming Inconel 718. *Mater. Sci. Eng. A* 2008, 478, 119–124.
49. Kang, H.; Dong, Z.; Zhang, W.; Xie, Y.; Peng, X. Laser Melting Deposition of a Porosity-Free Alloy Steel by Application of High Oxygen-Containing Powders Mixed with Cr Particles. *Vacuum* 2019, 159, 319–323.
50. Li, L. Repair of Directionally Solidified Superalloy GTD-111 by Laser-Engineered Net Shaping. *J. Mater. Sci.* 2006, 41, 7886–7893.

51. AlShaer, A.W.; Li, L.; Mistry, A. The Effects of Short Pulse Laser Surface Cleaning on Porosity Formation and Reduction in Laser Welding of Aluminium Alloy for Automotive Component Manufacture. *Opt. Laser Technol.* 2014, 64, 162–171.
52. Gao, W.; Zhao, S.; Wang, Y.; Liu, F.; Zhou, C.; Lin, X. Effect of Re-Melting on the Cladding Coating of Fe-based Composite Powder. *Mater. Des.* 2014, 64, 490–496.
53. Zhou, J.; Tsai, H. Effects of Electromagnetic Force on Melt Flow and Porosity Prevention in Pulsed Laser Keyhole Welding. *Int. J. Heat Mass Transf.* 2007, 50, 2217–2235.
54. Zhang, N.; Liu, W.; Deng, D.; Tang, Z.; Liu, X.; Yan, Z.; Zhang, H. Effect of Electric-Magnetic Compound Field on the Pore Distribution in Laser Cladding Process. *Opt. Laser Technol.* 2018, 108, 247–254.
55. Wang, D.; Liang, E.; Chao, M.; Yuan, B. Investigation on the Microstructure and Cracking Susceptibility of Laser-Clad V2O5 /NiCrBSiC Alloy Coatings. *Surf. Coat. Technol.* 2008, 202, 1371–1378.
56. Cloots, M.; Uggowitzner, P.J.; Wegener, K. Investigations on the Microstructure and Crack Formation of IN738LC Samples Processed by Selective Laser Melting Using Gaussian and Doughnut Profiles. *Mater. Des.* 2016, 89, 770–784.
57. Bidron, G.; Doghri, A.; Malot, T.; Fournier-Dit-Chabert, F.; Thomas, M.; Peyre, P. Reduction of the Hot Cracking Sensitivity of CM-247LC Superalloy Processed by Laser Cladding Using Induction Preheating. *J. Mater. Process. Technol.* 2020, 277, 116461.
58. Alizadeh-Sh, M.; Marashi, S.P.H.; Ranjbarnodeh, E.; Shoja-Razavi, R. Laser Cladding of Inconel 718 Powder on a Non-Weldable Substrate: Clad Bead Geometry-Solidification Cracking Relationship. *J. Manuf. Process.* 2020, 56, 54–62.
59. Ebrahimzadeh, H.; Farhangi, H.; Mousavi, S.A. Hot Cracking in Autogenous Welding of 6061-T6 Aluminum Alloy by Rectangular Pulsed Nd:YAG Laser Beam. *Weld. World* 2020, 64, 1077–1088.
60. Näkki, J.; Tuominen, J.; Vuoristo, P. Effect of Minor Elements on Solidification Cracking and Dilution of Alloy 625 Powders in Laser Cladding. *J. Laser Appl.* 2017, 29, 012014.
61. Bielenin, M.; Schmidt, L.; Schrickler, K.; Bergmann, J.P. Prevention of Solidification Cracking by Use of a Diode Laser Superposition in Pulsed Laser Beam Welding. *Proc. SPIE* 2019, 10911, 144009.
62. Wei, H.; Chen, J.S.; Wang, H.; Carlson, B.E. Thermomechanical Numerical Analysis of Hot Cracking During Laser Welding of 6XXX Aluminum Alloys. *J. Laser Appl.* 2016, 28, 022405.
63. Opprecht, M.; Garandet, J.-P.; Roux, G.; Flament, C.; Soulier, M. Solution to the Hot Cracking Problem for Aluminium Alloys Manufactured by Laser Beam Melting. *Acta Mater.* 2020, 197, 40–53.
64. Chen, L.; Zhang, X.; Wu, Y.; Chen, C.; Li, Y.; Zhou, W.; Ren, X. Effect of surface morphology and microstructure on the hot corrosion behavior of TiC/IN625 coatings prepared by extreme high-speed laser cladding. *Corros. Sci.* 2022, 201, 110271.